

Article

A Finite Element Stress Analysis of a Concical Triangular Connection in Implants: A New Proposal

Romy Angeles Maslucan ^{1,*}  and John Alexis Dominguez ²¹ School of Dentistry, Universidad Peruana Cayetano Heredia, Lima 15037, Peru² Department of Social Dentistry, School of Dentistry, Universidad Peruana Cayetano Heredia, Lima 15037, Peru; john.alexis.dominguez@upch.pe

* Correspondence: romy@amdentistas.com

Abstract: Conical implant–abutment connections are popular for their stability; however, in other conditions, such as excessive force, implants and abutments can absorb all the stress. Some connections with three points of support can resist more than conical connections. In recent years, different studies has shown that the design of a connection affects its stability. The aim of this study was to analyze and compare the stresses in finite elements (FEs) in a newly proposed conical triangular connection in implants with hexagonal and conical connections. A nonlinear 3D FE parametric model was developed using SOLIDWORKS 2017[®]. All the connections, i.e., external and internal hexagons, morse taper, conical connection, and the new conical triangular proposal were compared when axial forces of 150, 250, and 350 N were applied to the occlusal. The maximum stress was found in the external hexagon. The maximum stress was concentrated at the level of the neck of the abutment, implant, and bone, except for the morse taper; at the level of the crown and abutment, the lowest stress occurred in the new proposal. Conclusions: The new conical triangular (CT) connection and the conical connection (CC) generate similar stress in the implant, abutment, and crown. However, the CT connection improves the CC by reducing stress at the bone level, adding an advantage to having three retention points.

Keywords: finite element method; implant; new connection

Citation: Angeles Maslucan, R.; Dominguez, J.A. A Finite Element Stress Analysis of a Concical Triangular Connection in Implants: A New Proposal. *Materials* **2022**, *15*, 3680. <https://doi.org/10.3390/ma15103680>

Academic Editors: Giuliana Muzio and Gianmario Schierano

Received: 29 March 2022

Accepted: 16 May 2022

Published: 20 May 2022

Publisher's Note: MDPI stays neutral with regard to jurisdictional claims in published maps and institutional affiliations.



Copyright: © 2022 by the authors. Licensee MDPI, Basel, Switzerland. This article is an open access article distributed under the terms and conditions of the Creative Commons Attribution (CC BY) license (<https://creativecommons.org/licenses/by/4.0/>).

1. Introduction

One of the most popular treatments for edentulous patients is dental implants. The success of supported implant prostheses is based on the integration of implants with new bone (osseointegration) [1,2]. Studies have been carried out on the influence of masticatory forces in osseointegrated implants since the 1970s, by researchers who have evaluated the functional masticatory capacity in 165 patients with implants, finding values much higher than when they used a removable prosthesis [3–6].

The biomechanics of implant rehabilitations have been well studied through experimental and FEM (finite element method) studies. These connections (between the implant and the abutment) are affected by occlusal forces; considering that, when placing implants, due to the lack of periodontal ligament, the forces are transmitted through the implant and its components as stress that will finally cause a bone resorption [7–12].

There are several types of connections (triangular, hexagons, octagons, etc.), within which the internal connections have less stress than the external connections [13–20]. Within the internal connections, the “conical” type presents better results because it generates less stress as compared with other connections, which is associated with a lower bone resorption at the implant level, as indicated by studies conducted by Coelho et al. [21], which evaluated internal and conical hexagon connections by applying 200 N and found less stress in the conical connection as compared with the hexagonal connection when subjected to vertical forces [19–22].

Connections with three points of support such as the trichannel generate better stress distribution; however, not many studies have been found in reference to these [9–22]. Studies carried out by Coppedè et al. [7], Raoofi et al. [1], and Carvalho et al. [10] among others have suggested that conical connections with three points of support such as the trichannel better distributed the stress in the implant, therefore, in this study, we evaluated a new internal connection with a triangular conical design, which could generate a reduction in stress around the bone tissue surrounding the neck of the implant [8–10,18,21,23–43].

Sakka et al. [2] conducted a literature review on the factors associated with implant failures, among which the progressive loss of marginal bone and occlusal overforce could generate alterations at the level of the abutment implant connection. Likewise, Gehrke et al. [9] and Formiga et al. [7] studied types of MEF connections: conical, internal, and external hexagon, where the implants were subjected to axial and oblique forces of 100 N, and found that the overforces occurred between the connection of the implant with the abutment, which suggested that the design of the connection could be associated with bone resorption [10–12].

Currently, no scientific studies that refer to a conical triangular connection; however, Raoofi et al. [1] conducted MEF studies in different types of connections (hexagon, trichannel, and conical), and found that the internal trichannel type of connection generated less stress when applying axial forces of 300 N [22].

This research proposes a conical triangular connection, which is a new proposal for implant connection to reduce the stresses transmitted to the implant. Since we know that the type of implant connection could influence the transmission of forces to the bone surrounding the implant, the conical triangular connection could achieve a decrease in saucerization (marginal bone loss of 1.5 mm during the first year and 0.2 mm annually after the insertion of the prosthesis) [8–10,12].

The aim of this study was to analyze and compare the effects of occlusal load direction on the stress of implant-supported partial dentures manufactured within a new connection proposal, i.e., a conical triangular (CT) (Figure 1) connection versus hexagonal, Morse taper, and conical connections, with different axial forces, using a three-dimensional finite element analysis (FEA).

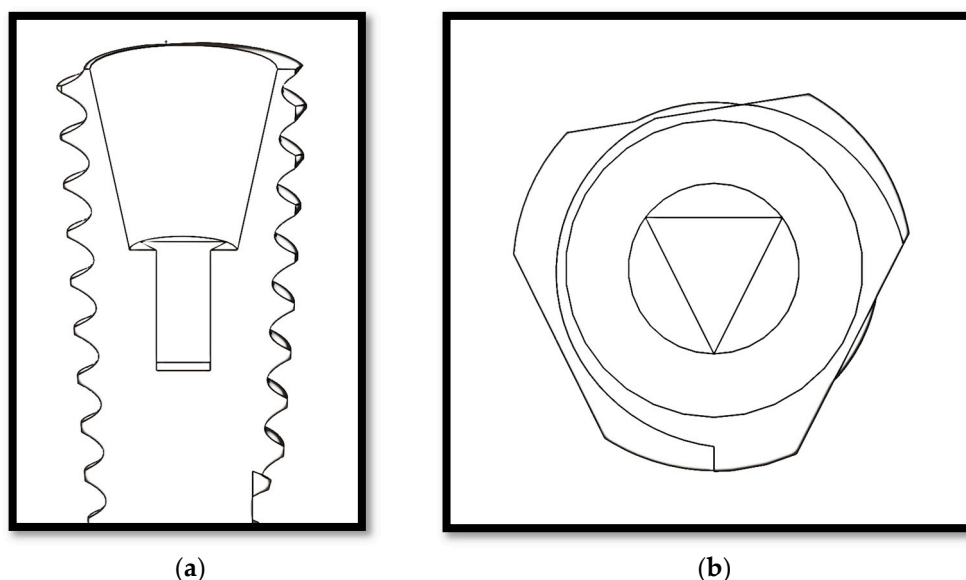


Figure 1. (a) Sagittal view of the CT connection; (b) occlusal view of the CT connection.

2. Materials and Methods

2.1. Finite Elements Model Studies

FEM studies determine through simulations the response of a body to limit situations (muscle, joint, and occlusal load) and its application in the dental field began more than

a decade ago; FEM studies are currently being applied in implantology to contribute databases by analyzing the stresses that implants support during masticatory forces. In 1976, Weinstein et al. [6] were the first to use FEM in implantology. Since then, several studies have used this method to evaluate components, connections, shapes, etc. [7–10,24,41–60]. These simulations resemble reality, in such a way that their results show a high level of reliability [6–10].

Three-dimensional finite elements based on solid element models were constructed that reproduced the clinical situation of an implant-supported upper premolar (SOLIDWORKS 3D CAD Design Software, Dassault Systèmes, SOLIDWORKS Corporation, Concord, MA, USA). The study group consisted of 15 models of grade 5 titanium implants with five different connection designs: external hexagon (EH), internal hexagon (IH), morse taper (MT), conical (CC), and conical triangular (CT) (Appendix A, Figure A1)). For each of the 5 implant connections, a 2 mm thick cortical bone block was modeled, and a fixed prosthesis supported by implants was designed to restore a porcelain upper premolar.

All implants were considered to be osseointegrated (bonding between the implant and surrounding bone was assumed [13]); they were designed with a diameter of 3.8×12 mm and placed at bone level. The implant–abutment connection systems varied for each model: EH, IH, MT, CC, and the new CT connection. Modeled prosthetic components were also integrated into the implant system. The bone–implant interface was assumed to be perfect, simulating complete osseointegration. Movement was restricted on the sides and on the lower areas, mimicking the real scenario of a dental implant placement into bone. Therefore, the connections between implant–cortical and implant–cancellous bones were designed to be bonded as well as the interface between cancellous and cortical bones. Within the implant system, FEM modeling was performed by implementing bonded conditions on the abutment–implant interfaces. The entire structure was held by setting all 6 degrees of freedom of mesiodistal surfaces of cancellous and cortical bones to zero. All the models were constructed using three-dimensional 4-node tetrahedral elements.

For all the models, the mesh type was solid standard mesh with 4 Jacobian points and quadratic elements of high order (i.e., fine mesh). The contact was global between components, and we considering that the implant was osseointegrated, the abutment fixed to the implant, and the crown was fixed to the abutment.

The boundary conditions for all models were established on both sides of the bone section. To analyze the maximum stress, axial axis of the implant forces was applied at the level of the occlusal surface of the palatine cusp (work cusp) of the upper premolar crown at forces of 150, 250, and 350 N (Figure 2).

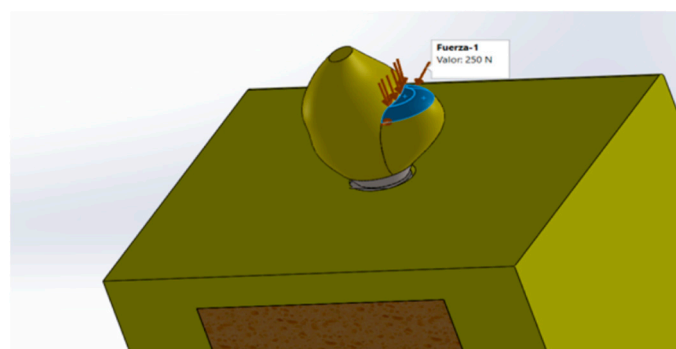


Figure 2. Application of forces at the occlusal side (palatal cuspid).

All materials were considered to be isotropic, homogeneous, and nonlinear. Considering the physical properties of each material (Table 1), the maximum and minimum von Mises stress values were determined for each model. The von Mises analysis showed a color scale, which allowed us to visualize, in red, the areas of greatest stress. The models were labeled according to the implant–abutment connection system (i.e., EH, IH, MT, CC, and CT).

Table 1. Mechanical proprieties used in finite element analyses.

Material	Young's Modul (MPa)	Poisson's Ratio (ν)	Reference(s)
Porcelain	68,900	0.28	De Carvalho Formiga et al. [9]
Titanium Alloy (Ti-6Al-4V)	110,000	0.35	De Carvalho Formiga et al. [9]; Yao, K.-T. et al. [61]
Cancellous Bone	1370	0.30	De Carvalho Formiga et al. [9]; Yao, K.-T. et al.
Cortical Bone	13,700	0.30	Yao K-T et al. [61]

2.2. Data Analysis

The von Mises stresses were used to present the stress values. A stress map was generated showing the stress distribution in the implants, abutments, crowns, and bone. Because this study was a simulation using FEA, no statistical analysis was necessary [60].

3. Results

The highest stress values were concentrated in the neck of the implant and cortical bone, except for the MT, where the maximum stress was concentrated at the middle of the implant and the bone (Appendix B).

When analyzing the maximum stress of the crown (43.5 and 10.1 MPa, respectively, with 350 N) and the abutment, the lowest values were obtained by the CC and the new CT proposal, and the highest value was the EH, followed by the IH and MT (Table 2).

Table 2. The von Misses stress in the connections.

Component	Crown			Abutment			
	Forces	150 N	250 N	350 N	150 N	250 N	350 N
EH		173	288	404	255	375	525
IH		48.9	81.5	114	58.2	97	136
MT		40.7	67.8	95	94	157	219
CC		18.7	31.1	43.5	4.3	7.17	10
CT		18.7	31.1	43.5	4.3	7.21	10.1
Component	Implant			Bone			
	Forces	150 N	250 N	350 N	150 N	250 N	350 N
EH		75	125	175	75.1	125	175
IH		11.9	19.8	27.8	0.26	0.44	0.617
MT		1.54	2.56	3.59	0.002	0.003	0.0053
CC		0.19	0.33	0.465	0.41	0.68	0.964
CT		0.63	1.06	1.49	0.3	0.5	0.7

EH, external hexagon; IH, internal hexagon; MT, morse taper; CC, conical connection; CT, conical triangular (new connection).

At the implant level, the CC and the newly proposed CT connection generated less stress (1.49 MPa with 350 N). When analyzing and comparing the maximum stress in the MT connection applying vertical forces of 150, 250, and 350 N, the highest stresses were obtained at both the level of the crown and the abutment; however, the MT connection had the lowest stress at the bone level (Appendix B, Figures A2, A3 and A5).

The number of elements ranged from 42,373 to 87,618 (Table 3) (CosmosWorks, Dassault Systèmes).

3.1. Stress at the Crown

In the CC and the new CT connection, the maximum stress was located on the occlusal face (Figure 3a), unlike the IH, EH, and MT (Figure 3b), where the stress was higher and concentrated at the level of the neck's crown.

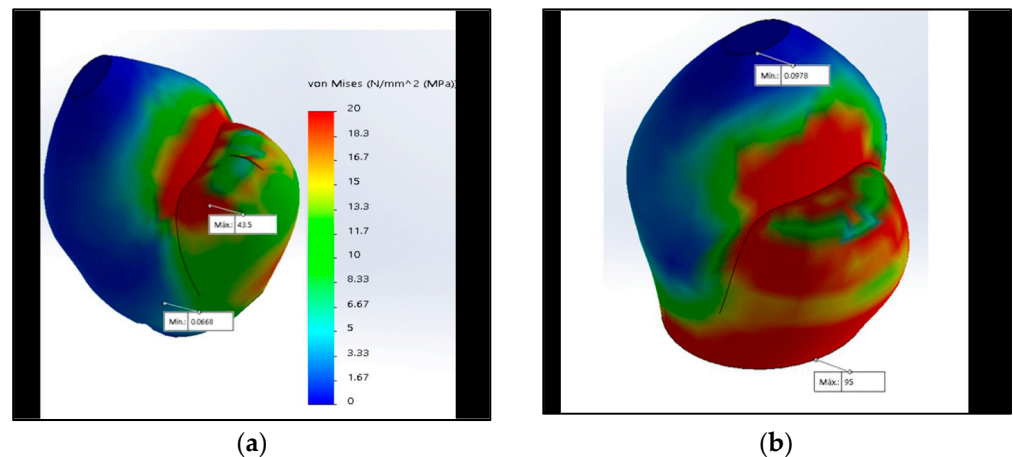


Figure 3. The maximum stress with 350 N at the crown is represented by red using the von Mises scale: (a) Maximum stress in the occlusal face in the CT connection; (b) maximum stress in the neck in the MT connection.

3.2. Abutment

The von Mises analysis of the abutment showed that the maximum stress in the MT and the newly proposed CT was concentrated at the level of the abutment's neck which supports the base of the crown, unlike the IH where the maximum stress was focused on the neck (Figure 4a).

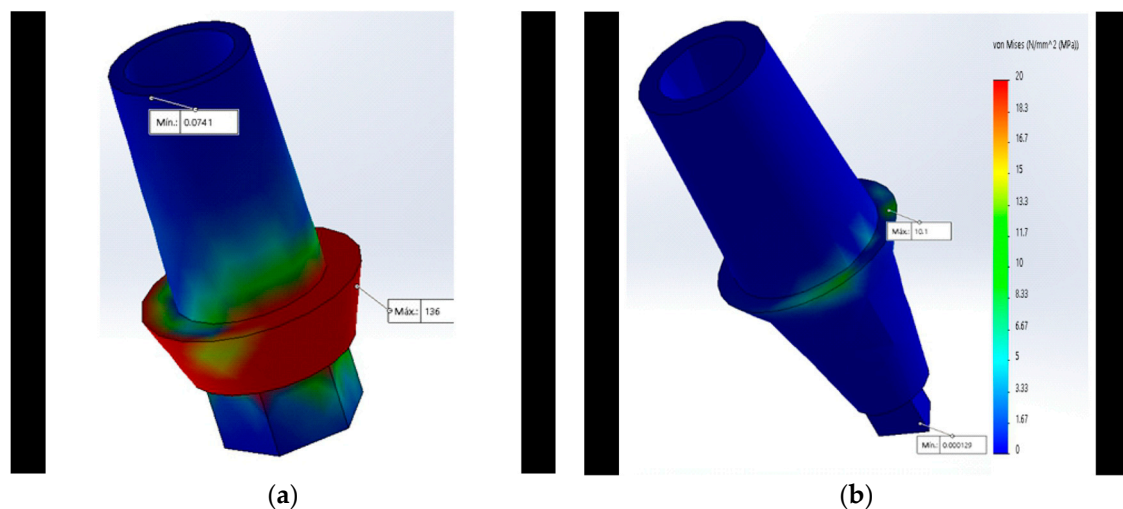


Figure 4. Maximum stress with 350 N at the abutment is represented by the red color using the von Mises scale: (a) Maximum stress at the neck in the IH connection; (b) maximum stress at the neck in the CT was lower (represented by the green color).

3.3. Implant

The von Mises analysis of the implant showed that the maximum stress in all designs except the MT (Figure 5a) was concentrated at the cervical level of the implant (Figure 5b).

3.4. Bone

When performing the von Mises analysis in the bone, it was observed that the maximum stress in all the designs, except for the MT, was concentrated at the neck level of the bone (Figure 6a–c). In the MT connection, the stress distribution was concentrated at the middle of the bone (Figure 6b), this being the same area of the maximum concentration of stress coinciding with the MT implant (Figure 5a).

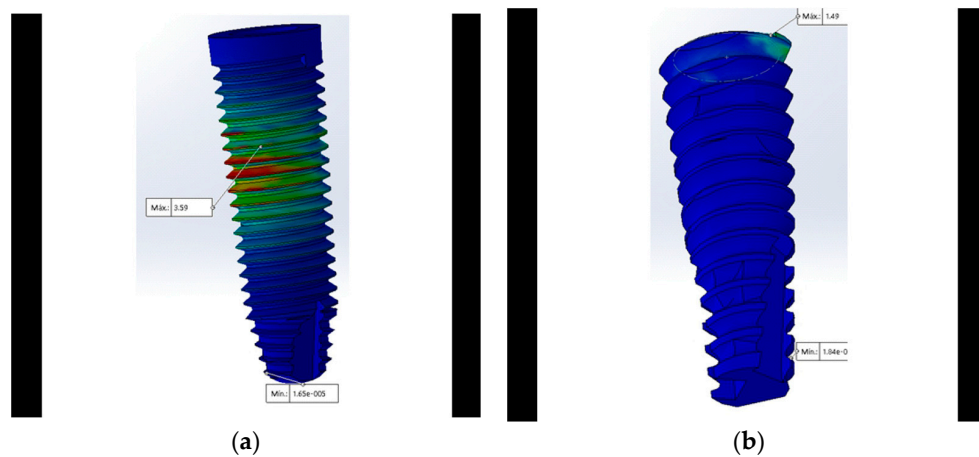


Figure 5. Maximum stress with 350 N in the implant is represented by the color red using the von Mises scale: (a) Maximum stress at the center in the MT connection; (b) maximum stress at the neck of the CT was lower (represented by the green color).

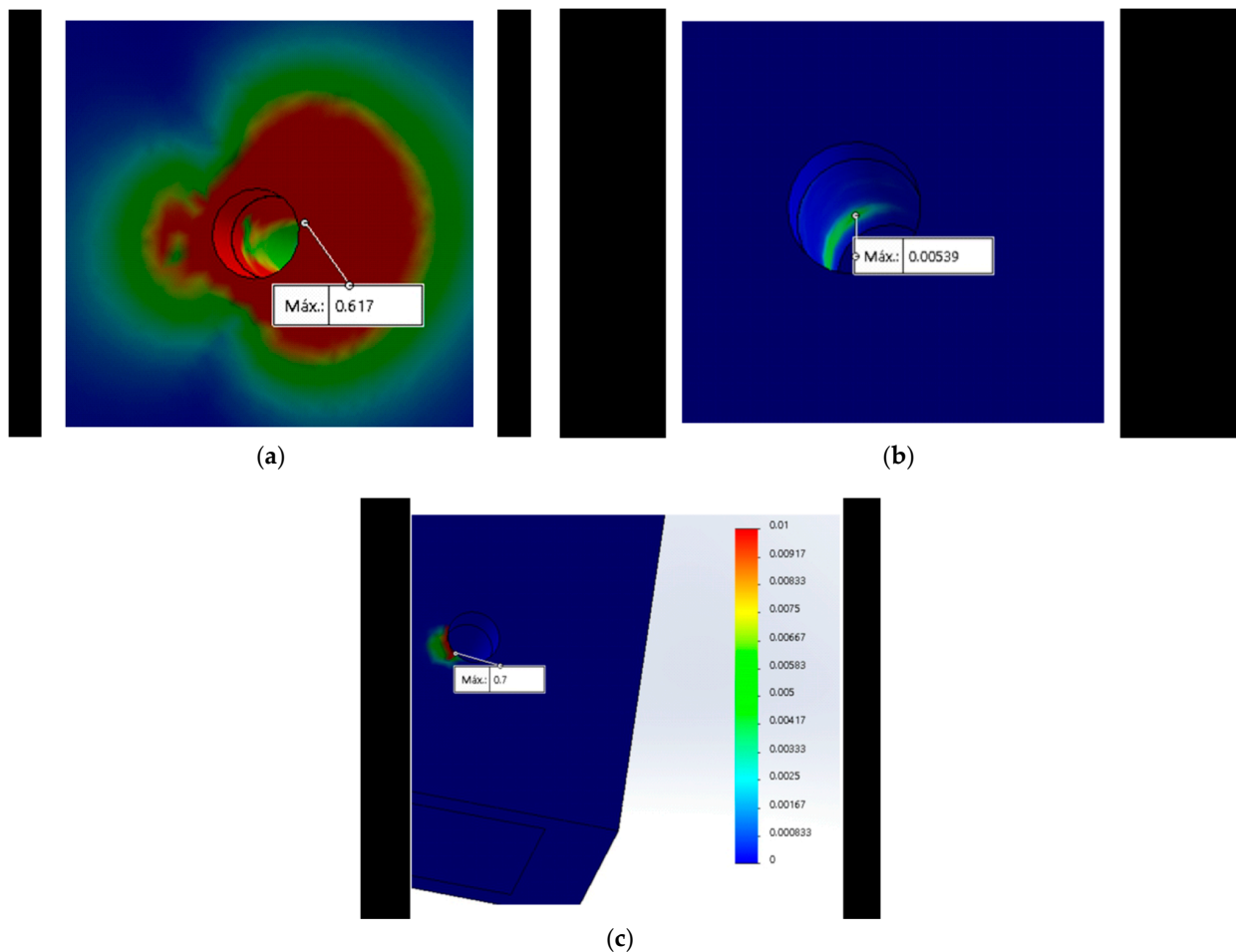


Figure 6. Maximum stress with 350 N in the bone is represented by the red color using the von Mises scale: (a) Maximum stress at the neck in the IH connection; (b) maximum stress at the middle in the MT connection; (c) maximum stress at the neck in the TC connection.

4. Discussion

Studies in FEM are simulations that help assess the effect of axial forces on dental implants and adjacent structures, as suggested by studies conducted by Raofi et al. [1],

Tabata et al. [10], Cho et al. [11], Borie et al. [12], Chun et al. [20], Baggi et al. [24], Quaresma et al. [25], Pessoa et al. [35], Eskitascioglu et al. [38], Siadat et al. [47], and Devaraju et al. [51], who performed analyses on FEs of implants to observe the biomechanical reactions and that of their adjacent structures. The characteristics of the number of elements (Table 3) are similar to the studies carried out by Siadat et al. [47], Raoofi et al. [1], and Cho et al. [11].

Table 3. Mesh characteristics.

Material	EH	IH	MT	CC	CT
Total number of nodes	61,529	102,590	120,983	120,174	127,650
Total number of items	42,373	70,200	78,599	82,528	87,618
% of distorted elements (Jacobian)	0	0	0	0	0
Item size	1.4 mm	1.16 mm	1.04 mm	1.03 mm	1.03 mm
Tolerance	0.07 mm	0.05 mm	0.05 mm	0.05 mm	0.05 mm

C. McNeill reported that, at the level of the anterior teeth, the forces received on the occlusal surface are between 100 and 150 N and, at the level of the first molar, the forces are between 300 N and 400 N on the crown [37]. Based on this, the forces of 150, 250, and 350 N were applied on the supported implant crowns.

In all designs except the MT, it was found that maximum stress was concentrated at the level of the neck of the implant and bone, which was also reflected in the implant abutments; this was comparable to studies carried out by Sutpideler et al. [57], Kitamura et al. [58], and Borie et al. [12], where they found that the highest concentration of stress was at the cervical bone and implant level.

The external hexagon: The connection that generated the greatest stress in the bone, implant, and its components was the EH. This was corroborated both by this study and studies carried out by Gehrke et al. [9] and Siadat et al. [47]. This was comparable to studies by Esposito, Tsouknidas, and Gehrke, who evaluated compressive forces and torques between external and internal hexagonal connections, and found that the EH generated greater torque and stress [9,46–48].

In the present study, the IH improved the external hexagon; thus, our results were similar to the studies carried out by Siadat et al. [47] and Lemus Cruz et al. [21], who evaluated microfiltration and torque and found better torque resistance to the internal hexagon connection. Although this design improved on the external hexagon, the IH generated greater stress than the newly proposed CT connection at the implant and component level.

Morse Taper: The maximum von Mises stress found in the bone was less than 0.01 MPa. This was comparable to studies conducted by Devaraju et al. and Fiorillo et al. [51], who analyzed the distribution of stress with 800 N. The results obtained with the MT connection, similar to this study, generated less stress; probably because of its morphology and conical design [7,16,21,31,32,34,47,54,59,60].

The conical Connection: The lowest stress at the level of the implants, abutment, and crown occurred in the conical connection design and in the new conical triangular (CT) connection. As shown in Table 2, this was consistent with studies conducted by Coppédé et al. [5] and [21,22], where conical connection dental implants had lower stress than the internal hexagon [25].

The Conical Triangular connection: The studies carried out by Coppédé et al., Raoofi et al. and Formiga et al., among others, suggested that conical connections in addition to three points of support, such as the proposed CT, distributed stress better in implants.

In spite of that, the CT produced similar stress to that of the CC in all components; at the bone level, even with a high value of 350 N, the stress value was 0.7 MPa (Table 2). The new CT connection generated lower stress in the bone than the CC.

The results obtained in this study provide information that helps in making decisions when evaluating the type of implant connection for patients [49], and there is less potential

for fractures in the components of the CT because of its geometry (an equilateral triangle on the base of conical connection) [1].

The morse taper continues to show less stress in the bone, however, this type of connection generated more stress in both: the abutment and the crown as compared with the CC and CT connections.

Although, clinically, the internal hexagon has more positions for the abutment as compared with the new CT proposal, when we analyzed the results at the pillar level, the IH obtained more than 200% (150 N: IH, 94 MPa and CT, 4.3 MPa) and, in the crown, the maximum stress in the IH was double as compared with the CT proposal (Table 2). This justifies, from an engineering point of view, the possibility of low stress and deformation in the three-channel design due to the triangular distribution of the load over other connection designs [7–9], within the limitations of this study and considering the assumptions made for these FE models. It should be noted that this study was static and only analyzed the forces in work cuspid; therefore, it is recommended that future similar studies apply a study in dynamics to evaluate fatigue and, thus, observe how implant designs behave under cyclic loads.

5. Conclusions

The stress in the new conical triangular connection is similar to the CC, both were lower at the level of the crown, abutment, and implant as compared with the EH, IH, and MT connections. Likewise, although the lowest stress at the bone level was in the MT connection, the maximum stress in the new CT connection was less than 1 MPa.

The CT connection as an alternative could be the first Peruvian implant connection that could compete with similar foreign implants, offering a more accessible treatment as an innovative treatment. These three support points have less potential for component fractures because of their geometry.

The results of this study present theoretical and social importance, because we evaluated the influence of design in the implant connection and its stresses distribution in the implant and the surrounding bone; and we determined that CT and CC are the most conservative and longevity treatment option for our patients.

Although the hexagon has more possibilities of positions for the abutment, at the level of the implant, the hexagon generates more stress than the conical connection and the conical triangular connection. Taking into consideration the finding by Borie et al. [14] who showed that when a load was applied to an implant it was partially transferred to the bone, CT could be an option for patients with parafunction such as bruxism.

The present study shows that the new CT connection is viable, since it presents lower stress on the implant with similar values to that of CC; both connections obtain less stress in the abutment and crown than conventional connections. Furthermore, the CT connection improves the CC at bone level. For this reason, it is an alternative for both specialists in implantology and dental prosthetists.

6. Patents

This new conical triangular connection has a patent in Peru and is also published in Google patents. <https://patents.google.com/patent/PE20210771Z/en?q=romy+angeles&dq=romy+angeles> (accessed on 24 March 2022).

Author Contributions: Conceptualization, R.A.M. and J.A.D.; methodology, R.A.M. and J.A.D.; validation, R.A.M. and J.A.D.; formal analysis, R.A.M. and J.A.D.; investigation, R.A.M. and J.A.D.; resources, R.A.M.; writing—original draft preparation, R.A.M. and J.A.D.; writing—review and editing, R.A.M., J.A.D. and MDPI author services (<https://www.mdpi.com/authors/english>) (accessed on 24 March 2022); supervision, J.A.D.; project administration, R.A.M. and J.A.D. All authors have read and agreed to the published version of the manuscript.

Funding: This research received no external funding.

Institutional Review Board Statement: This study was conducted in accordance with the University Direction of Research, Science, and Technology, approved by the Universidad Peruana Cayetano Heredia, and this research project was submitted to SIDISI (Decentralized Research Information and Monitoring System (<https://investigacion.cayetano.edu.pe/registro/sidisi>) (accessed on 14 January 2019)) with no. 101513. This study did not involve humans or animals; however, this study was passed by an ethics committee for exoneration at the Universidad peruana Cayetano Heredia on 15 January 2019.

Informed Consent Statement: Not applicable.

Data Availability Statement: The data is available on <https://repositorio.upch.edu.pe/handle/20.500.12866/10027>.

Acknowledgments: My thanks to my thesis advisor John Alexis Domínguez for his support with the research, as well as to Marisol Castilla.

Conflicts of Interest: The authors declare no conflict of interest.

Appendix A

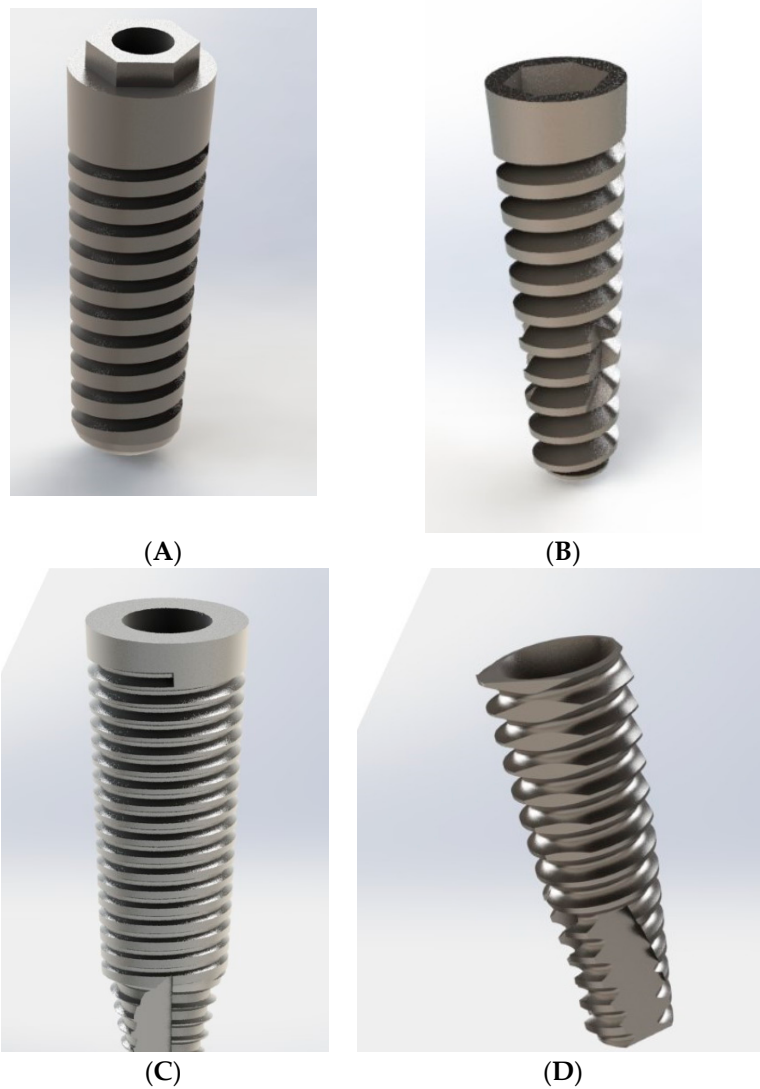


Figure A1. Cont.

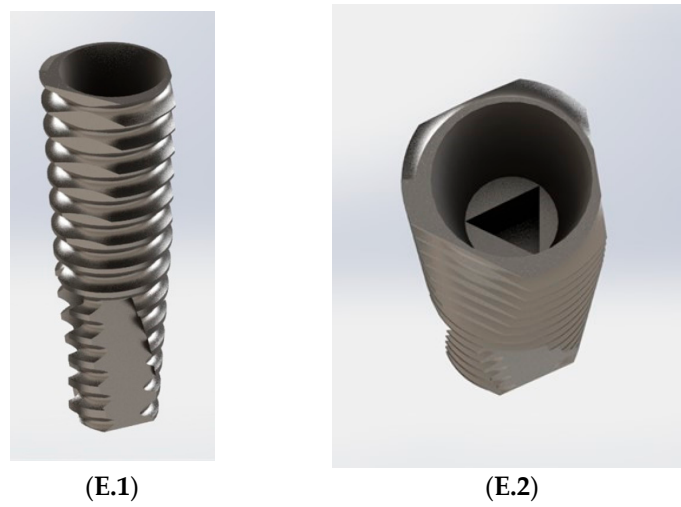


Figure A1. Five models of implant connections: (A) External hexagon; (B) internal hexagon; (C) morse taper; (D) conical; (E.1) conical triangular lateral view; (E.2) conical triangular occlusal view.

Appendix B

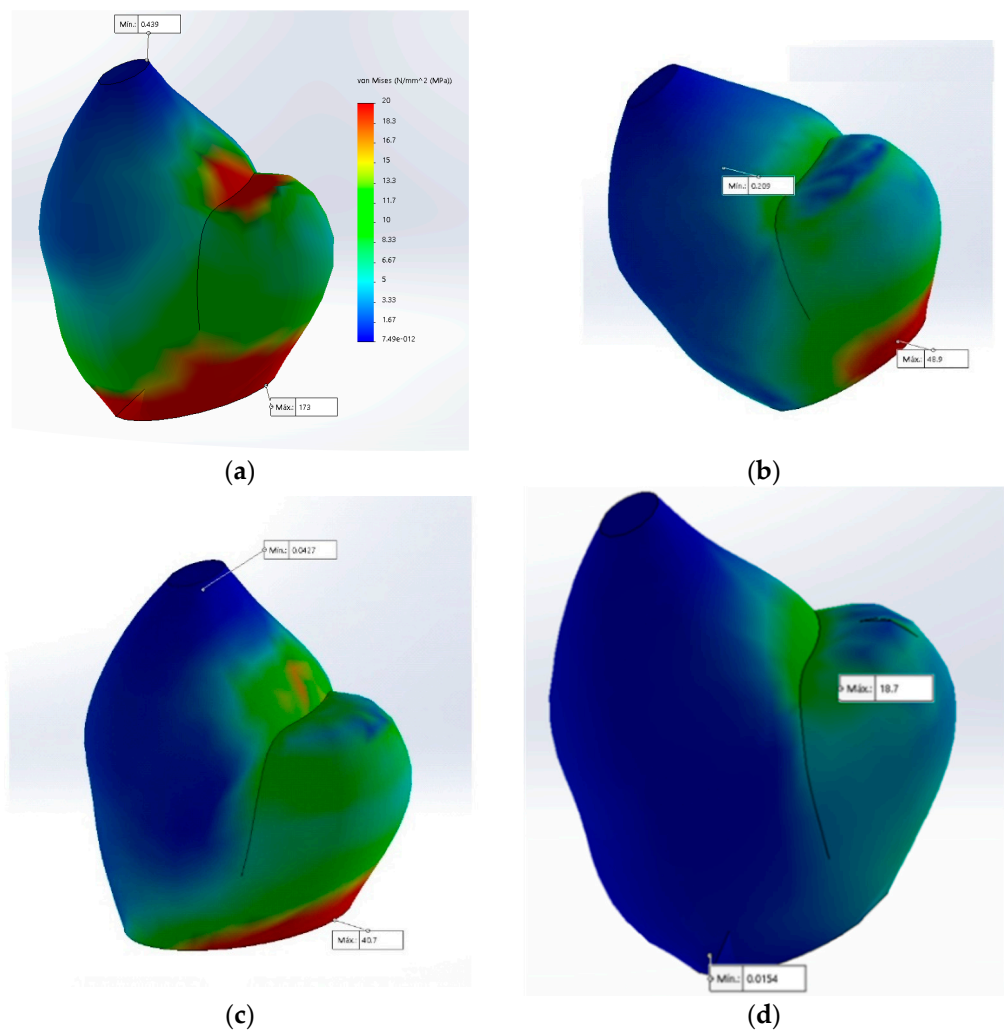


Figure A2. Cont.

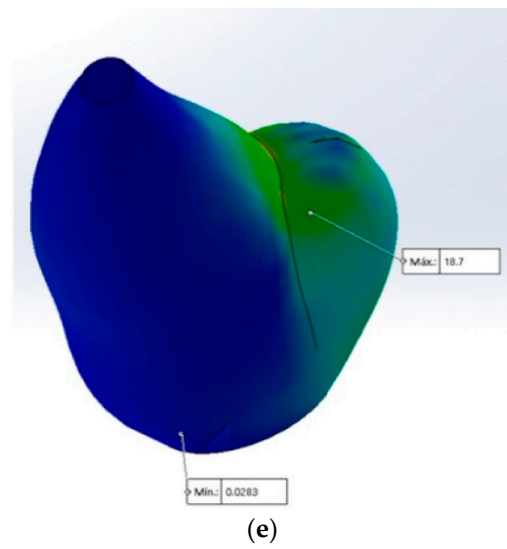


Figure A2. Maximum Stress in the crown with 150 N in connections: (a) External hexagon; (b) internal hexagon; (c) morse taper; (d) conical connection; (e) conical triangular connection.

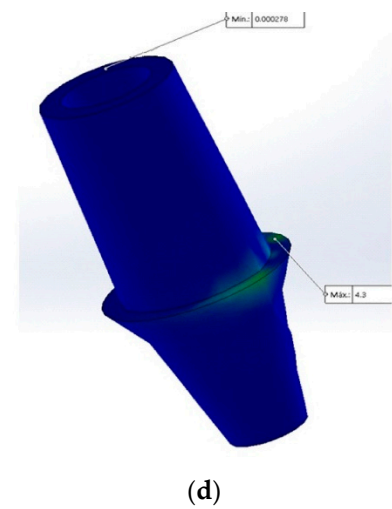
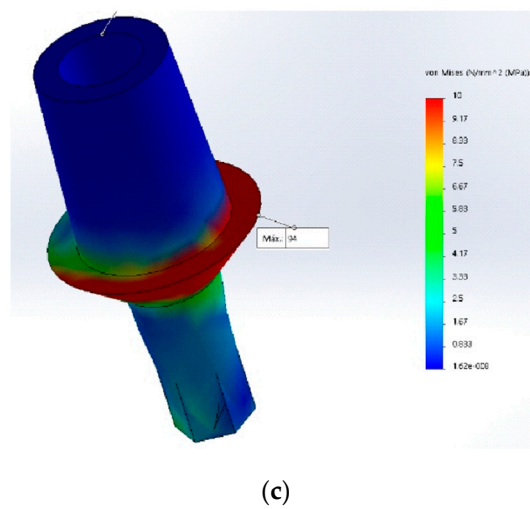
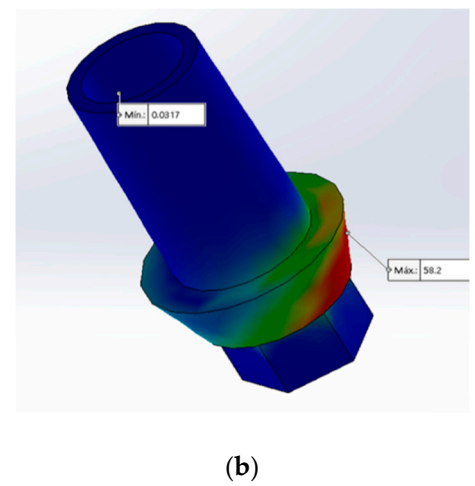
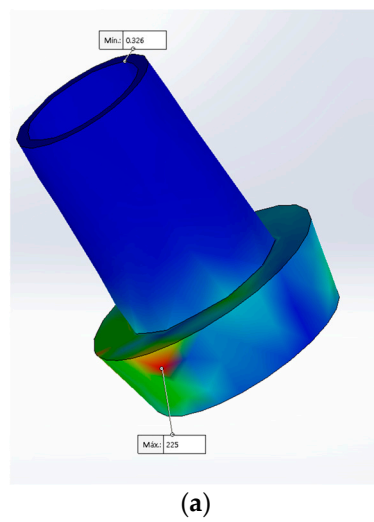


Figure A3. Cont.

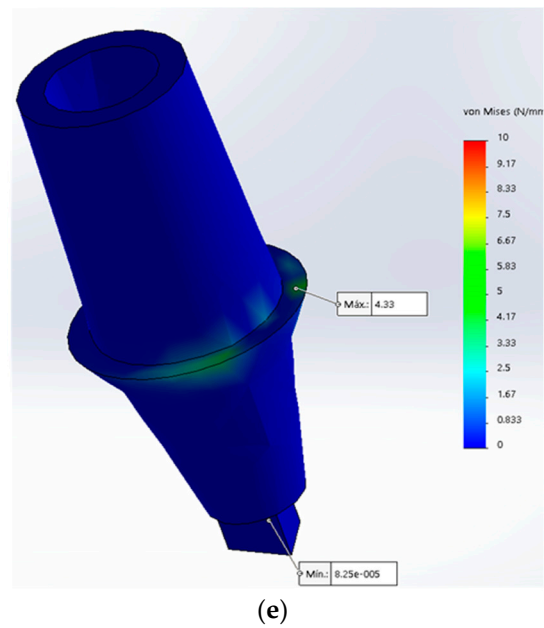


Figure A3. Maximum stress in the abutment with 150 N: (a) External hexagon; (b) internal hexagon; (c) morse taper; (d) conical connection; (e) conical triangular connection.

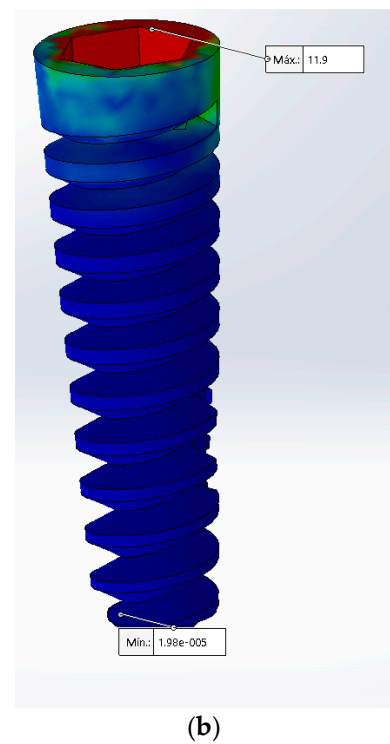
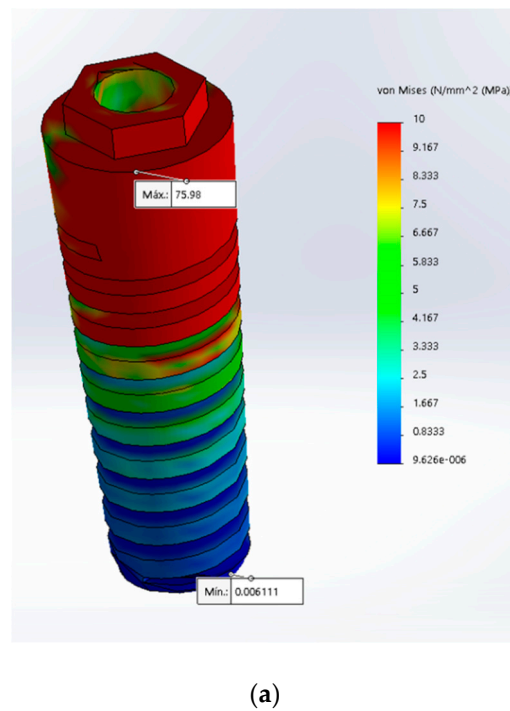


Figure A4. Cont.

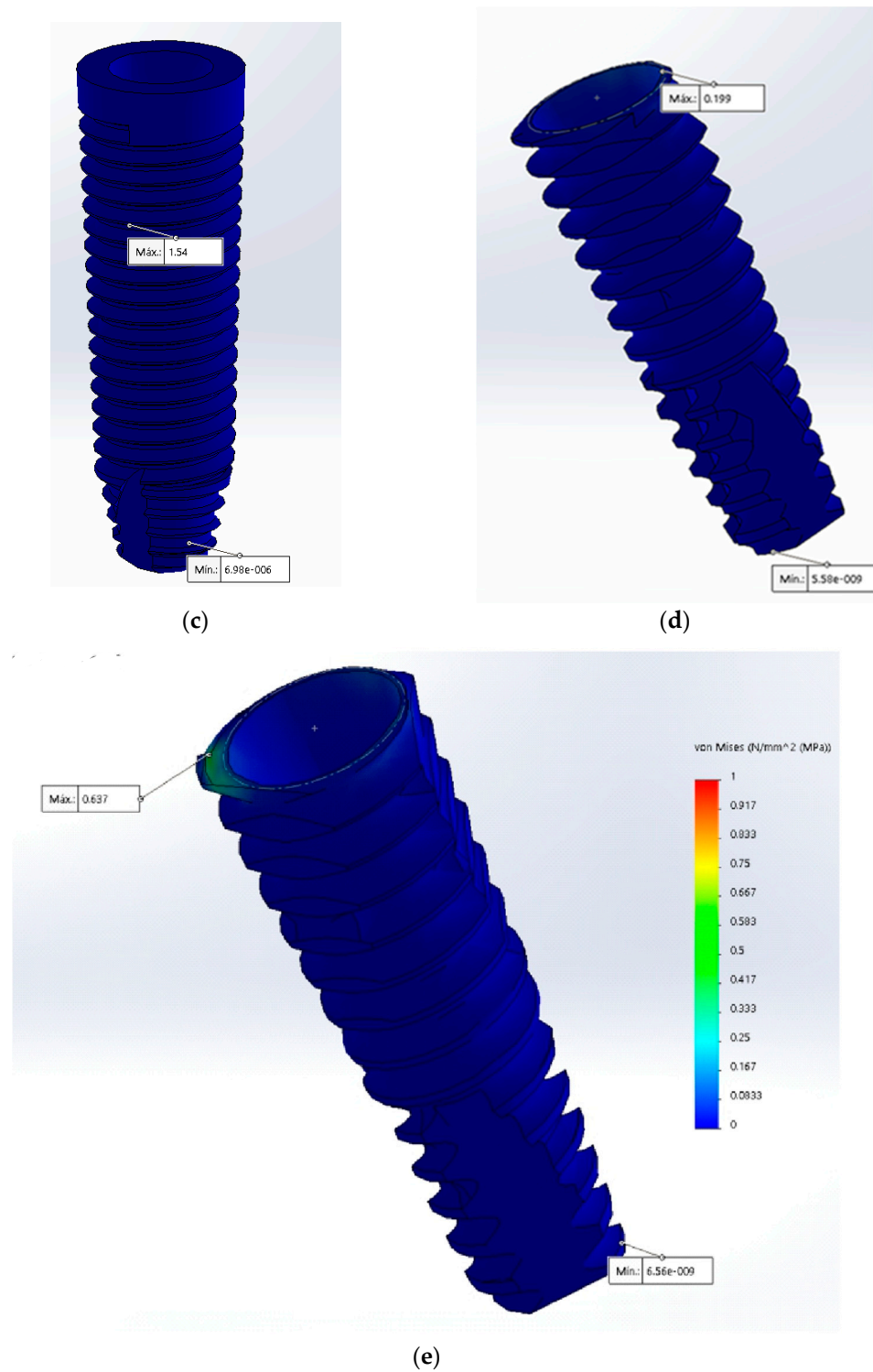


Figure A4. Maximum stress in the implant with 150 N: (a) External hexagon; (b) internal hexagon; (c) morse taper; (d) conical connection; (e) conical triangular connection.

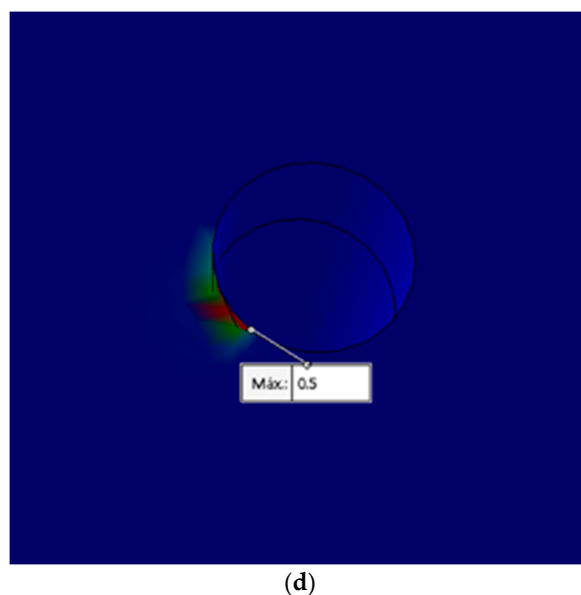


Figure A5. Maximum stress in the bone with 150 N: (a) Internal hexagon; (b) morse taper; (c) conical connection; (d) conical triangular connection.

References

1. Raoofi, S.; Khademi, M.; Amid, R.; Kadkhodazadeh, M.; Movahhedi, M.R. Comparison of the Effect of Three Abutment-implant Connections on Stress Distribution at the Internal Surface of Dental Implants: A Finite Element Analysis. *J. Dent. Res. Dent. Clin. Dent. Prospect.* **2013**, *7*, 132–139. [[CrossRef](#)]
2. Sakka, S.; Baroudi, K.; Nassani, M.Z. Factors Associated with Early and Late Failure of Dental Implants. *J. Investig. Clin. Dent.* **2012**, *3*, 258–261. [[CrossRef](#)] [[PubMed](#)]
3. Consolaro, A.; de Carvalho, R.S.; Francischone, C.E., Jr.; Consolaro, M.F.M.O.; Francischone, C.E. Saucerização de Implantes Osseointegrados e o Planejamento de Casos Clínicos Ortodônticos Simultâneos. *Dent. Press J. Orthod.* **2010**, *15*, 19–30. [[CrossRef](#)]
4. Weinstein, A.M.; Klawitter, J.J.; Anand, S.C.; Schuessler, R. Stress Analysis of Porous Rooted Dental Implants. *J. Dent. Res.* **1976**, *55*, 772–777. [[CrossRef](#)]
5. Pesqueira, A.A.; Goiato, M.C.; Filho, H.G.; Monteiro, D.R.; dos Santos, D.M.; Haddad, M.F.; Pellizzer, E.P. Use of Stress Analysis Methods to Evaluate the Biomechanics of Oral Rehabilitation with Implants. *J. Oral Implantol.* **2014**, *40*, 217–228. [[CrossRef](#)]
6. Ricciardi Coppedè, A.; Lapria Faria, A.C.; Chiarello de Mattos, M.d.G.; Silveira Rodrigues, R.C.; Shibli, J.A.; Faria Ribeiro, R. Mechanical Comparison of Experimental Conical-Head Abutment Screws with Conventional Flat-Head Abutment Screws for External-Hex and Internal Tri-Channel Implant Connections: An In Vitro Evaluation of Loosening Torque. *Int. J. Oral Maxillofac. Implant.* **2013**, *28*, e321–e329. [[CrossRef](#)]
7. Formiga, M. Evaluation Using FEM on the Stress Distribution on the Implant, Prosthetic Components and Crown, with Cone Morse, External and Internal Hexagon Connections. *Dent. Press Implantol.* **2013**, *7*, 67–75.
8. Bechelli, A.H. *Carga Imediata em Implantologia Oral: Protocolos Diagnósticos, Quirúrgicos e Protéticos; Casos Clínicos*; Providence: Buenos Aires, Argentina, 2006.
9. Gehrke, S.; Junior, J.; Dedavid, B.; Shibli, J. Analysis of Implant Strength After Implantoplasty in Three Implant-Abutment Connection Designs: An In Vitro Study. *Int. J. Oral Maxillofac. Implant.* **2016**, e65–e70. [[CrossRef](#)]
10. Tabata, L.F.; Rocha, E.P.; Barão, V.A.R.; Assunção, W.G. Platform Switching: Biomechanical Evaluation Using Three-Dimensional Finite Element Analysis. *Int. J. Oral Maxillofac. Implant.* **2011**, *26*, 482–491.
11. Cho, S.-Y.; Huh, Y.-H.; Park, C.-J.; Cho, L.-R. Three-Dimensional Finite Element Analysis of the Stress Distribution at the Internal Implant-Abutment Connection. *Int. J. Periodontics Restor. Dent.* **2016**, *36*, e49–e58. [[CrossRef](#)]
12. Borie, E.; Orsi, I.; Noritomi, P.; Kemmoku, D. Three-Dimensional Finite Element Analysis of the Biomechanical Behaviors of Implants with Different Connections, Lengths, and Diameters Placed in the Maxillary Anterior Region. *Int. J. Oral Maxillofac. Implant.* **2016**, *31*, 101–110. [[CrossRef](#)] [[PubMed](#)]
13. Anami, L.C.; da Costa Lima, J.M.; Takahashi, F.E.; Neisser, M.P.; Noritomi, P.Y.; Bottino, M.A. Stress Distribution Around Osseointegrated Implants With Different Internal-Cone Connections: Photoelastic and Finite Element Analysis. *J. Oral Implantol.* **2015**, *41*, 155–162. [[CrossRef](#)] [[PubMed](#)]
14. Flanagan, D.; Phillips, J.; Connor, M.; Dyer, T.; Kazerounian, K. Hoop Stress and the Conical Connection. *J. Oral Implantol.* **2015**, *41*, 37–44. [[CrossRef](#)] [[PubMed](#)]
15. Lee, J.-H.; Kim, D.-G.; Park, C.-J.; Cho, L.-R. Axial Displacements in External and Internal Implant-Abutment Connection. *Clin. Oral Implant. Res.* **2014**, *25*, e83–e89. [[CrossRef](#)] [[PubMed](#)]

16. Schmitt, C.M.; Nogueira-Filho, G.; Tenenbaum, H.C.; Lai, J.Y.; Brito, C.; Döring, H.; Nonhoff, J. Performance of Conical Abutment (Morse Taper) Connection Implants: A Systematic Review. *J. Biomed. Mater. Res. A* **2014**, *102*, 552–574. [CrossRef]
17. Coppedè, A.R.; Bersani, E.; de Mattos, M.d.G.C.; Rodrigues, R.C.S.; Sartori, I.A.d.M.; Ribeiro, R.F. Fracture Resistance of the Implant-Abutment Connection in Implants with Internal Hex and Internal Conical Connections under Oblique Compressive Loading: An in Vitro Study. *Int. J. Prosthodont.* **2009**, *22*, 283–286.
18. Davi, L.R.; Golin, A.L.; Bernardes, S.R.; de Araújo, C.A.; Neves, F.D. In Vitro Integrity of Implant External Hexagon after Application of Surgical Placement Torque Simulating Implant Locking. *Braz. Oral Res.* **2008**, *22*, 125–131. [CrossRef]
19. Vigolo, P.; Fonzi, F.; Majzoub, Z.; Cordioli, G. Evaluation of Gold-Machined UCLA-Type Abutments and CAD/CAM Titanium Abutments with Hexagonal External Connection and with Internal Connection. *Int. J. Oral Maxillofac. Implant.* **2008**, *23*, 247–252.
20. Chun, H.-J.; Shin, H.-S.; Han, C.-H.; Lee, S.-H. Influence of Implant Abutment Type on Stress Distribution in Bone under Various Loading Conditions Using Finite Element Analysis. *Int. J. Oral Maxillofac. Implant.* **2006**, *21*, 195–202.
21. Pessoa, R.S.; Coelho, P.G.; Muraru, L.; Marcantonio, E.; Vaz, L.G.; Vander Sloten, J.; Jaecques, S.V.N. Influence of Implant Design on the Biomechanical Environment of Immediately Placed Implants: Computed Tomography-Based Nonlinear Three-Dimensional Finite Element Analysis. *Int. J. Oral Maxillofac. Implant.* **2011**, *26*, 1279–1287.
22. Lemus Cruz, L.M.; Almagro Urrutia, Z.; Claudia León Castell, A. Origen y Evolucion de Los Implantes Dentales. *Rev. Habanera Cienc. Médicas* **2009**, *8*.
23. Dos, A. Biomechanical Study of Prosthetic Interfaces: A Literature Review. Available online: <https://www.semanticscholar.org/paper/Biomechanical-study-of-prosthetic-interfaces-%3A-A-Do%C5%9F/ec44f07a2b432f689ad1076a1772095c533024f8> (accessed on 16 February 2022).
24. Gazzotti, P.D.; Endruhn, A. *La Rehabilitacion Implanto-Protésica*; Providence: Buenos Aires, Argentina, 2011.
25. Baggi, L.; Cappelloni, I.; Di Girolamo, M.; Maceri, F.; Vairo, G. The Influence of Implant Diameter and Length on Stress Distribution of Osseointegrated Implants Related to Crestal Bone Geometry: A Three-Dimensional Finite Element Analysis. *J. Prosthet. Dent.* **2008**, *100*, 422–431. [CrossRef]
26. Quaresma, S.E.T.; Cury, P.R.; Sendyk, W.R.; Sendyk, C. A Finite Element Analysis of Two Different Dental Implants: Stress Distribution in the Prosthesis, Abutment, Implant, and Supporting Bone. *J. Oral Implantol.* **2008**, *34*, 1–6. [CrossRef]
27. Gardner, D.M. Platform Switching as a Means to Achieving Implant Esthetics. *N. Y. State Dent. J.* **2005**, *71*, 34–37.
28. Mangano, C.; Bartolucci, E.G. Single Tooth Replacement by Morse Taper Connection Implants: A Retrospective Study of 80 Implants. *Int. J. Oral Maxillofac. Implant.* **2001**, *16*, 675–680.
29. Gil, F.J.; Aparicio, C.; Manero, J.M.; Padros, A. Influence of the Height of the External Hexagon and Surface Treatment on Fatigue Life of Commercially Pure Titanium Dental Implants. *Int. J. Oral Maxillofac. Implant.* **2009**, *24*, 583–590.
30. Shi, L.; Li, H.; Fok, A.S.L.; Ucer, C.; Devlin, H.; Horner, K. Shape Optimization of Dental Implants. *Int. J. Oral Maxillofac. Implant.* **2007**, *22*, 911–920.
31. Abu-Hammad, O.A.; Harrison, A.; Williams, D. The Effect of a Hydroxyapatite-Reinforced Polyethylene Stress Distributor in a Dental Implant on Compressive Stress Levels in Surrounding Bone. *Int. J. Oral Maxillofac. Implant.* **2000**, *15*, 559–564.
32. Sakoh, J.; Wahlmann, U.; Stender, E.; Nat, R.; Al-Nawas, B.; Wagner, W. Primary Stability of a Conical Implant and a Hybrid, Cylindric Screw-Type Implant in Vitro. *Int. J. Oral Maxillofac. Implant.* **2006**, *21*, 560–566.
33. Mangano, C.; Mangano, F.; Piattelli, A.; Iezzi, G.; Mangano, A.; La Colla, L. Prospective Clinical Evaluation of 307 Single-Tooth Morse Taper-Connection Implants: A Multicenter Study. *Int. J. Oral Maxillofac. Implant.* **2010**, *25*, 394–400.
34. Zambrano, M.E.A.; Reina, A.C.; Domínguez, G.C.; Fernández, D.A.G.; Fábrega, J.G. Biomecánica en implantología. *Periodoncia Osteointegración* **2005**, *15*, 311–326.
35. Pessoa, R.S.; Muraru, L.; Júnior, E.M.; Vaz, L.G.; Sloten, J.V.; Duyck, J.; Jaecques, S.V.N. Influence of Implant Connection Type on the Biomechanical Environment of Immediately Placed Implants—CT-Based Nonlinear, Three-Dimensional Finite Element Analysis. *Clin. Implant Dent. Relat. Res.* **2009**, *12*, 219–234. [CrossRef] [PubMed]
36. Chu, C.-M.; Huang, H.-L.; Hsu, J.-T.; Fuh, L.-J. Influences of Internal Tapered Abutment Designs on Bone Stresses Around a Dental Implant: Three-Dimensional Finite Element Method With Statistical Evaluation. *J. Periodontol.* **2012**, *83*, 111–118. [CrossRef] [PubMed]
37. Karl, M.; Winter, W.; Taylor, T.D.; Heckmann, S.M. In Vitro Study on Passive Fit in Implant-Supported 5-Unit Fixed Partial Dentures. *Int. J. Oral Maxillofac. Implant.* **2004**, *19*, 30–37.
38. McNeill, C. *Fundamentos Científicos y Aplicaciones Prácticas de la Oclusión*; Quintessence: Barcelona, Spain, 2005.
39. Eskitascioglu, G.; Usumez, A.; Sevimay, M.; Soykan, E.; Unsal, E. The Influence of Occlusal Loading Location on Stresses Transferred to Implant-Supported Protheses and Supporting Bone: A Three-Dimensional Finite Element Study. *J. Prosthet. Dent.* **2004**, *91*, 144–150. [CrossRef]
40. Misch, C.E. *Implantología Contemporánea*; Elsevier: New York, NY, USA, 2009.
41. Linck, G.K.S.B.; Ferreira, G.M.; De Oliveira, R.C.G.; Lindh, C.; Leles, C.R.; Ribeiro-Rotta, R.F. The Influence of Tactile Perception on Classification of Bone Tissue at Dental Implant Insertion. *Clin. Implant Dent. Relat. Res.* **2016**, *18*, 601–608. [CrossRef]
42. Cícero Dinato, J.; Daudt Polido, W. *Implantes Oseointegrados: Cirugía y Prótesis*; Artes Médicas: Sao Paulo, Brasil, 2003.
43. Beltrán, V.; Into, F.R.P.; Amos, G.d.G.R.; Iotti, D.; So, L.B. Switching Platform on Esthetic Area: Case Report. *Dent. Press Implantol.* **2012**, *6*, 93–103.

44. Pellizzer, E.P.; Verri, F.R.; Falcón-Antenucci, R.M.; Júnior, J.F.S.; de Carvalho, P.S.P.; de Moraes, S.L.D.; Noritomi, P.Y. Stress Analysis in Platform-Switching Implants: A 3-Dimensional Finite Element Study. *J. Oral Implantol.* **2012**, *38*, 587–594. [[CrossRef](#)]
45. Hong, H.R.; Pae, A.; Kim, Y.; Paek, J.; Kim, H.-S.; Kwon, K.-R. Effect of Implant Position, Angulation, and Attachment Height on Peri-Implant Bone Stress Associated with Mandibular Two-Implant Overdentures: A Finite Element Analysis. *Int. J. Oral Maxillofac. Implant.* **2012**, *27*, e69–e76.
46. Huiskes, R.; Chao, E.Y. A Survey of Finite Element Analysis in Orthopedic Biomechanics: The First Decade. *J. Biomech.* **1983**, *16*, 385–409. [[CrossRef](#)]
47. Hurtado, J.E.; Jorge, E. Análisis de elementos finitos estocásticos por estimaciones puntuales y expansión espectral. *Rev. Int. Métod. Numér. Para Cálculo Diseño Ing.* **2001**, *17*, 305–316.
48. Siadat, H.; Najafi, H.; Alikhasi, M.; Falahi, B.; Beyabanaki, E.; Zayeri, F. Effect of Lateral Oblique Cyclic Loading on Microleakage and Screw Loosening of Implants with Different Connections. *J. Dent. Res. Dent. Clin. Dent. Prospects* **2018**, *12*, 183–189. [[CrossRef](#)] [[PubMed](#)]
49. Fiorillo, L.; Cicciù, M.; D’Amico, C.; Mauceri, R.; Oteri, G.; Cervino, G. Finite Element Method and Von Mises Investigation on Bone Response to Dynamic Stress with a Novel Conical Dental Implant Connection. *BioMed Res. Int.* **2020**, *2020*, 2976067. [[CrossRef](#)] [[PubMed](#)]
50. Prados-Privado, M.; Gehrke, S.A.; Rojo, R.; Prados-Frutos, J.C. Complete Mechanical Characterization of an External Hexagonal Implant Connection: In Vitro Study, 3D FEM, and Probabilistic Fatigue. *Med. Biol. Eng. Comput.* **2018**, *56*, 2233–2244. [[CrossRef](#)] [[PubMed](#)]
51. Hsu, P.-F.; Yao, K.-T.; Kao, H.-C.; Hsu, M.-L. Effects of Axial Loading on the Pull-out Force of Conical Connection Abutments in Ankylos Implant. *Int. J. Oral Maxillofac. Implant.* **2018**, *33*, 788–794. [[CrossRef](#)]
52. Devaraju, K.; Rao, S.; Joseph, J.; Raju Kurapati, S. Comparison of Biomechanical Properties of Different Implant-Abutment Connections. *Indian J. Dent. Sci.* **2018**, *10*, 180. [[CrossRef](#)]
53. Kanneganti, K.; Vinnakota, D.; Pottem, S.; Pulagam, M. Comparative Effect of Implant-Abutment Connections, Abutment Angulations, and Screw Lengths on Preloaded Abutment Screw Using Three-Dimensional Finite Element Analysis: An in Vitro Study. *J. Indian Prosthodont. Soc.* **2018**, *18*, 161. [[CrossRef](#)]
54. Massoumi, F.; Taheri, M.; Mohammadi, A.; Amelirad, O. Evaluation of the Effect of Buccolingual and Apicocoronal Positions of Dental Implants on Stress and Strain in Alveolar Bone by Finite Element Analysis. *J. Dent. Tehran Iran* **2018**, *15*, 10–19.
55. Lehmann, R.B.; Elias, C.N.; Zucareli, M.A. Influence of external geometry of Morse dental implant on stress distribution. *Dent. Press Implantol.* **2012**, *6*, 35–43.
56. Krennmair, G.; Seemann, R.; Schmidinger, S.; Ewers, R.; Piehslinger, E. Clinical Outcome of Root-Shaped Dental Implants of Various Diameters: 5-Year Results. *Int. J. Oral Maxillofac. Implant.* **2010**, *25*, 357–366.
57. Pereira, J.; Morsch, C.; Henriques, B.; Nascimento, R.; Benfatti, C.; Silva, F.; López-López, J.; Souza, J. Removal Torque and Biofilm Accumulation at Two Dental Implant–Abutment Joints After Fatigue. *Int. J. Oral Maxillofac. Implant.* **2016**, *31*, 813–819. [[CrossRef](#)] [[PubMed](#)]
58. Sütpideler, M.; Eckert, S.E.; Zobitz, M.; An, K.-N. Finite Element Analysis of Effect of Prosthesis Height, Angle of Force Application, and Implant Offset on Supporting Bone. *Int. J. Oral Maxillofac. Implant.* **2004**, *19*, 819–825.
59. Kitamura, E.; Stegaroiu, R.; Nomura, S.; Miyakawa, O. Influence of Marginal Bone Resorption on Stress around an Implant—A Three-Dimensional Finite Element Analysis. *J. Oral Rehabil.* **2005**, *32*, 279–286. [[CrossRef](#)] [[PubMed](#)]
60. Magomedov, I.A.; Khaliev, M.S.-U.; Elmurzaev, A.A. Application of Finite Element Analysis in Medicine. *J. Phys. Conf. Ser.* **2020**, *1679*, 022057. [[CrossRef](#)]
61. Yao, K.-T.; Chen, C.-S.; Cheng, C.-K.; Fang, H.-W.; Huang, C.-H.; Kao, H.-C.; Hsu, M.-L. Optimization of the Conical Angle Design in Conical Implant–Abutment Connections: A Pilot Study Based on the Finite Element Method. *J. Oral Implantol.* **2018**, *44*, 26–35. [[CrossRef](#)]